

Analytical models for the asymmetric wake of vertical axis wind turbines

Pablo Ouro^{a,b,*}, Maxime Lazenec^c

^a*School of Mechanical, Aerospace and Civil Engineering, University of Manchester, Manchester, M13 9PL, UK*

^b*Hydro-environmental Research Centre, School of Engineering, Cardiff University, Cardiff, CF24 3AA, UK*

^c*École Polytechnique, 91120 Palaiseau, Paris, France*

Abstract

Arrays of Vertical Axis Wind Turbines (VAWTs) can achieve larger power generation per land area than horizontal axis turbines farms, due to the positive synergy between VATs in close proximity. Theoretical wake models enable the reliable design of the array layout that maximises the energy output, which need to depict the driving wake dynamics. VAWTs generate a highly complex wake that evolves according to two governing length-scales, namely the turbine rotor's diameter and height which define a rectangular shape of the wake cross-section, and feature distinct wake expansion rates. This paper presents analytical VAWT wake models that account for an asymmetric distribution of such wake expansion adopting a top-hat and Gaussian velocity deficit distribution. Our proposed analytical Gaussian model leads to an enhanced initial wake expansion prediction with the wake width (ε) behind the rotor equal to $(\beta/4\pi)^{1/2}$ with β being the ratio of initial wake area to the VAWT's frontal area, which addresses the limitations of previous models that under-predicted the wake onset area. Velocity deficit predictions are calculated in a series of numerical benchmarks consisting of a single and an array of four in-line vertical axis wind turbines. In comparisons with field data and large-eddy simulations, our models provide a good accuracy to represent the mean wake distribution, maximum velocity deficit, and mo-

*Corresponding author: Dr Pablo Ouro (pablo.ouro@manchester.ac.uk)

Email addresses: pablo.ouro@manchester.ac.uk (Pablo Ouro), maxime.lazenec@polytechnique.edu (Maxime Lazenec)

mentum thickness, with the Gaussian model attaining the best predictions. These models will aid to drive the design of VAT arrays and accelerate this technology.

Keywords: Vertical Axis Wind Turbines, Wakes, Self-similarity, Large-Eddy Simulation, Wind farm, VAWT

1. Introduction

In the global landscape of wind energy generation, all large-scale wind farm projects comprise Horizontal Axis Wind Turbines (HAWTs) as a well-established technology for both onshore and offshore environments, becoming one of the most cost-effective resources to harness renewable energy [1]. Conversely, Vertical Axis Wind Turbines (VAWTs) are being developed at a much slower pace with the remaining main challenge to prove their financial viability, conditioned by the need for enhancing their power generation capabilities. VAWTs offer a series of advantages over their HAWT counterparts that can lead to innovative wind and hydro-kinetic energy projects, unfeasible if HAWTs were the chosen technology. For instance, they can effectively harness kinetic energy from relatively low-to-medium flow velocity ranges as those found in urban areas, rivers or tides, or be adopted in environmentally sensitive regions as their slower rotational speeds can reduce fish collision risk or acoustic contamination.

VAWT rotor blades rotate in a plane perpendicular to the approaching flow direction, generating vortex structures over the upwind rotation half and interacting with these over the downwind one. Despite such fluid-structure complexity of VAT wakes, the research in characterising VAWT wakes is still insufficient with limited knowledge about the governing flow mechanisms in the far-wake dynamics. This led to extrapolate features of HAT wakes into the dynamics of VAWT wakes which are fundamentally unequal, e.g. tip or dynamic-stall vortices patterns [2].

Most experimental tests of VATs look at how to improve their performance, leading to a limited number of studies analysing the near-wake dynamics and an almost absence of extensive tests that investigate the far-wake. Few examples of the latter at small-scale laboratory scale are: Rolin and Porté-Agel [3] measured with Particle Image Velocimetry (PIV) up to 10 diameters (D_0) downstream of a VAT analysing the mean and turbulent kinetic energy equations; Araya et al. [4] investigated the near- to far-wake

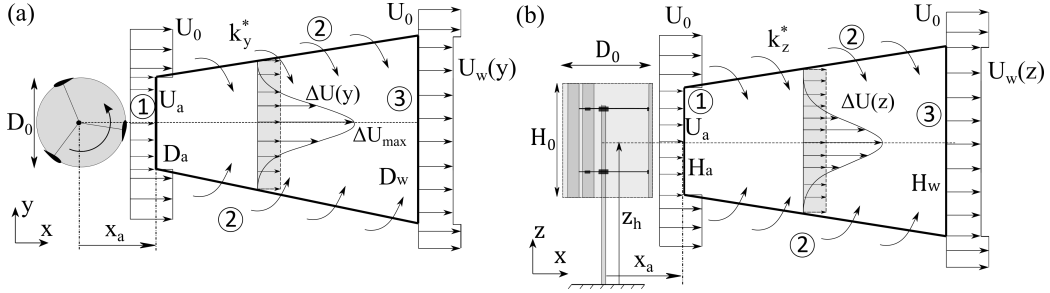


Figure 1: Wake evolution behind a VAWT of diameter D_0 and height H_0 over the (a) horizontal (xy) plane at a mid-height elevation z_h from the ground surface, and (b) vertical (xz) plane through the rotor's centre, with the thick solid line denoting the control volumes of interest.

transition for turbine rotors with different number of blades and tip-speed ratios using PIV to measure up to $11D_0$ downstream; and Ouro et al. [5] measured the wake up to $14D_0$ downstream with acoustic Doppler velocimeter showing that remnants of the turbine-induced wake are still observed at such far distances downstream.

The complex fluid dynamics in VAT wakes depend on the operational regime accounted for by the Tip-Speed Ratio (TSR) which relates the blades' angular speed to the free-stream velocity, and the turbine's rotor geometric solidity, which indicates the proportion of the swept perimeter occupied by the blades [6, 7]. VAWTs designed with low solidity rotors operate at high TSR which leads the blades to undergo light dynamic stall, i.e. flow separation occurs for effective angles of attacks larger than the static stall angle but there is no full detachment of the generated leading-edge vortices preventing a sudden drop in lift and torque. Alternatively, rotors with a higher solidity operate at low TSR and blades experience deep dynamic stall, meaning the attached leading-edge vortices enhance the lift-generation capabilities of the blades but at a given angle that is normally when torque generation is maximum these energetic vortices are shed [8, 7]. Whilst the latter configurations are common for Vertical Axis Tidal Turbines (VATTs), the design of VAWTs normally adopt with a low solidity rotor and attain their optimal TSR, i.e. relative rotational speed at which their power coefficient is maximum, in the range of 4–5 [9], but these may suffer from self-starting issues. Hence, designers are adopting more compact, higher solidity rotors that operate at optimal TSR ranges of approx. 1.5–2.5, which is mostly adopted in VATTs for hydro-kinetic applications at sea or in rivers [10, 8, 11].

The horizontal-to-vertical asymmetric distribution of VAWT wakes is depicted in Fig. 1, which considers a control volume behind a turbine with diameter D_0 and height H_0 over which mass and momentum needs to be conserved [12]. Over the horizontal xy -plane, the main contribution to momentum entrainment over the lateral boundaries of the control volume results from the blade-induced energetic vortices [13]. This differs from the wake recovery dynamics over the xz -vertical plane (Fig. 1b), as shear layers generated in this direction result from the tip vortices [9]. These blade-induced structures are not identical leading to potentially dissimilar wake mixing rates over the horizontal (k_y^*) and vertical (k_z^*) planes, causing an asymmetric wake recovery. Furthermore, VAWT rotors with height-to-diameter aspect ratio different to unity leads to having two length-scales with which the wake dynamics, e.g. velocity distributions, can be characterised, unlike HAWT wakes that scale with its diameter [14]. As shown in Fig. 1, in the horizontal plane D_0 is the characteristic length scale while in the vertical plane this is H_0 .

More insights into the complex turbulence structures generated by vertical axis wind or tidal rotor blades were gained from numerical simulations. Research has evidenced the need for eddy-resolving closures, such as Large-Eddy Simulation (LES), to resolve the flow within the VAT rotor and its wake, as Reynolds-Averaged Navier Stokes models can fail to predict dynamic stall [15] or the replenishment of mean kinetic energy in the wake which is driven by turbulence fluctuations [11, 5, 16]. Such flow complexity requires fine numerical grids with three approaches mostly adopted to represent VAT rotors. Geometry-resolved simulations, e.g. adopting an immersed boundary method, provide a high-resolution at the rotor capturing the vortices induced by the blades [17, 8]. Actuator techniques enable to adopt lower grid resolution while capturing the main wake dynamics but fail at representing the dynamic stall vortices [18]. Actuator Line Method (ALM) is the most widely adopted [19, 20, 21] whilst the Actuator Surface Method (ASM) can provide further gains to improve the resolution of the flow at rotor level [22].

There is still a need for developing analytical wake models tailored to VATs that enable its prediction at almost no computational cost [23], which is the aim of this article. Analytical models are widely adopted to design array layouts by industry and researchers as they enable the evaluation of multiple operational scenarios within a reasonable time frame [24], thus the presented models will be invaluable for the future design of VAT arrays [25].

Our models improve the wake expansion both in terms of expansion rate and wake onset area, and account for an asymmetric wake recovery, relevant for VATs with height-to-diameter aspect ratios different to unity. The structure of the paper is: §2 describes the underpinning basis our wake models are built upon, which are derived in §3. Validation in four cases with comparisons to large-eddy simulation results, field data and other available models are presented in §4, with the main conclusions drawn in §5.

2. Novelty of wake models

The underpinning physics of our models for VAWT wakes lie in considering the wake to expand according to two length-scales, namely the wake diameter (D_w) and height (H_w), featuring a rectangular shape analogously to the projected area of the VAWT ($A_0 = D_0 H_0$), as shown in Fig. 1. The cross-sectional wake area $A_w = D_w H_w$ at any downstream location (x) is determined as the evolution of the wake from its onset location, x_a , corresponding to the location at which pressure equilibrium is reached, i.e. the pressure at the wake centre is the same as the free-stream one. The latter needs to be downstream of the swept perimeter region, i.e. $x/D_0 \geq 0.5$, and for simplicity we set $x_a = 0.5D_0$ as the location of the wake onset in our models, analogously to the hypothesis done in HAT wake models in which such pressure equilibrium is attained almost immediately downstream of the turbine rotor Frandsen et al. [26].

The wake expansion is determined from two non-dimensional parameters corresponding to the horizontal (k_y) and vertical (k_z) directions, whose values can be dissimilar as the shear layers generated by tip vortices over the vertical direction are different to those from dynamic-stall vortices on the horizontal one. Our wake expansion considerations allow to develop a Gaussian wake model that accounts for a physically valid estimation of the initial wake area, addressing limitations found in other VAT models partly build upon concepts from HAWT wakes whose under-prediction of the wake area at x_a leads to non-physical values of velocity deficit in the near-wake, as discussed in §4. Note that from hereafter we will use VAT to avoid distinction of wind or tidal turbines as models can be applicable to either of these.

3. Derivation of the wake models

3.1. Momentum conservation

We build our momentum conserving wake models starting from the conservation form of the Reynolds Averaged Navier-Stokes equation for high Reynolds numbers in the streamwise direction. After neglecting the pressure and viscous terms, this equation reads

$$\frac{\partial U_w(U_0 - U_w)}{\partial x} + \frac{\partial V_w(U_0 - U_w)}{\partial y} + \frac{\partial W_w(U_0 - U_w)}{\partial z} = \frac{\partial u'u'}{\partial x} + \frac{\partial u'v'}{\partial y} + \frac{\partial u'w'}{\partial z} \quad (1)$$

with (U_w, V_w, W_w) being the vector of mean wake velocities in the streamwise, transverse and vertical directions respectively, and $u'u'$, $u'v'$ and $u'w'$ denote time-averaged turbulent fluctuation correlations. We integrate 1 at any streamwise location of a control volume that embeds the turbine and expands over the y and z directions from $-\infty$ to ∞ , which together with the assumption the shear stresses vanish when increasing the distance from the wake centre provides the resulting RANS equation,

$$\frac{d}{dx} \int_{-\infty}^{\infty} (U_w (U_0 - U_w) - u'u') dA \approx 0 \quad (2)$$

The streamwise variation of $u'u'$ is much reduced when compared to the convective term [12], hence 2 can be simplified to obtain the momentum integral [27] as

$$\rho \int_{-\infty}^{\infty} (U_w (U_0 - U_w)) dA = T \quad (3)$$

This equilibrium condition states that the momentum deficit flux in the wake is proportional to the thrust force T exerted by the turbine. Note that we consider the wakes to be in zero-pressure gradient flow and the incoming velocity to be mostly uniformly distributed in the three directions of space. The thrust force can be related to the thrust coefficient (C_T) from the actuator disk theory as

$$T = \frac{1}{2} C_T \rho A_0 U_0^2 \quad (4)$$

3.2. Top-hat wake model

The value of the wake onset area A_a can be determined using the actuator disk theory as $A_a = \beta A_0$, with β representing the relative initial wake expansion at x_a in terms of the turbine rotor's cross-section A_0 , independently of whether such cross-section is circular (HATs) or rectangular (VATs). The actuator disk theory states the velocity over the plane at x_a is $U_0(1 - 2a)$ whilst at the rotor centre plane the velocity is $U_0(1 - a)$, with $a = \frac{1}{2}(1 - \sqrt{1 - C_T})$ being the so-called induction factor. Hence, the value of β is determined based on energy conservation as:

$$\beta = \frac{A_a}{A_0} = \frac{1 - a}{1 - 2a} = \frac{1}{2} \frac{1 + \sqrt{1 - C_T}}{\sqrt{1 - C_T}} \quad (5)$$

The wake area at any streamwise location is determined similarly to the approach presented by Frandsen et al. [26] for HATs with $D_w \propto x^{1/2}$. Hence, the wake width is considered to expand asymmetrically over the horizontal and vertical directions as:

$$D_w = D_0 \left(\beta + k_{wy} \frac{x - x_a}{D_0} \right)^{1/2}, \quad H_w = H_0 \left(\beta + k_{wz} \frac{x - x_a}{H_0} \right)^{1/2} \quad (6)$$

We now apply momentum balance to a control volume that embeds the operating turbine expanding some distance upstream and downstream to obtain the velocity deficit $\Delta U = U_0 - U_w$ for the top-hat model with asymmetric expansion over the horizontal and vertical directions:

$$\frac{\Delta U}{U_0} = \frac{1}{2} \left(1 - \sqrt{1 - \frac{2C_T}{\left(\beta + k_{wy} \frac{x - x_a}{D_0} \right)^{1/2} \left(\beta + k_{wz} \frac{x - x_a}{H_0} \right)^{1/2}}} \right) \quad (7)$$

Values of k_{wy} and k_{wz} are considered equal to $2.0I_u$, with I_u denoting streamwise turbulence intensity. This value is half the one adopted in HAT wakes [26] and in other VAT wake models [28]. We propose this value as it provides better predictions of momentum thickness or maximum ΔU as shown later in §4.

3.3. Gaussian wake model

A cornerstone in the derivation of a Gaussian wake model is to assume the velocity deficit distribution to be self-similar, i.e. at any streamwise

distance ΔU can be directly determined from local scales of velocity and length [27]. For axisymmetric wakes, as is the case of HAT wakes [29], self-similarity is attained if the transverse distribution of ΔU consistently follows a given function $f(-\frac{1}{2}(r/\sigma)^2)$, where r/σ is the distance from the wake centre (r) normalised by the characteristic wake width (σ); and a given velocity scale $C(x)$, which is determined as the maximum normalised velocity deficit ($\Delta U_{max}/U_0$) at any streamwise distance. The self-similar normalised ΔU can be written as

$$\frac{\Delta U}{U_0} = \frac{U_0 - U_w}{U_0} = C(x)f\left(-\frac{1}{2}\frac{r^2}{\sigma^2}\right) \quad (8)$$

We assume ΔU to be self-similar following a Gaussian shape function, with results in §4 showing this condition is deemed valid. Adopting a Gaussian distribution allows a more physically-realistic description of the wake velocity deficit compared to top-hat models that assume a uniform value across the wake width. Whilst in most HAT wake cases the self-similar shape function is defined only by the turbine diameter [30, 31], for VATs both its diameter and height are characteristic length-scales that determine the distribution of $\Delta U/U_0$ over the horizontal and vertical directions of the wake. The wake asymmetry is accounted in our model by adopting the superposition of two Gaussian distributions $\Delta U(y)$ and $\Delta U(z)$, whose characteristic wake widths σ_y and σ_z scale depending on D_0 and H_0 , respectively. Following Bastankhah and Porté-Agel [12], we propose these wake widths to expand linearly in the downwind direction:

$$\frac{\sigma_y}{D_0} = k_y^* \frac{x - x_a}{D_0} + \varepsilon_y \quad , \quad \frac{\sigma_z}{H_0} = k_z^* \frac{x - x_a}{H_0} + \varepsilon_z \quad (9)$$

Wake expansion rates k_y^* and k_z^* are estimated as $0.35I_u$ as proposed by Bastankhah and Porté-Agel [12], which are proven adequate given the wake predictions presented in §4 considering ε_y and ε_z that represent the wake onset width are well determined. The wake velocity 8 can be re-written as

$$U_w = U_0 \left(1 - C(x) \exp\left(-\frac{y^2}{2\sigma_y^2} - \frac{z^2}{2\sigma_z^2}\right) \right) \quad (10)$$

This is an algebraic equation with one unknown, the velocity scale $C(x)$, which is solved equating the momentum integral 3 to the turbine thrust force 4 to obtain the definition of the wake velocity 10 as

$$\begin{aligned}
& \int_{-\infty}^{\infty} U_0^2 C(x) \exp\left(-\frac{y^2}{2\sigma_y^2} - \frac{z^2}{2\sigma_z^2}\right) \left(1 - C(x) \exp\left(-\frac{y^2}{2\sigma_y^2} - \frac{z^2}{2\sigma_z^2}\right)\right) dA \\
&= \frac{1}{2} C_T A_0 U_0^2
\end{aligned} \tag{11}$$

Considering the rectangular cross-section of the wakes $A_w = D_w H_w$ and $\int_{-\infty}^{\infty} \exp(-y^2/(2\sigma_y^2)) dy = \sqrt{2\pi}\sigma_y$ and $\int_{-\infty}^{\infty} \exp(-y^2/\sigma_y^2) dy = \sqrt{\pi}\sigma_y$, 11 can be integrated to determine the normalised maximum velocity deficit, $C(x)$, as

$$\sigma_y \sigma_z \pi C(x)^2 - 2\pi \sigma_y \sigma_z C(x) + \frac{1}{2} C_T A_0 = 0 \tag{12}$$

From the two possible solutions to this quadratic equation, the value that provides a physical solution for the characteristic velocity scale is then

$$C(x) = \frac{\Delta U_{max}}{U_0} = 1 - \sqrt{1 - \frac{C_T A_0}{2\pi \sigma_y \sigma_z}} \tag{13}$$

Our proposed Gaussian model for VAT wakes is obtained from 10 and 13 as

$$\frac{\Delta U}{U_0} = \left(1 - \sqrt{1 - \frac{C_T D_0 H_0}{2\pi \sigma_y \sigma_z}}\right) \exp\left(-\frac{y^2}{2\sigma_y^2} - \frac{z^2}{2\sigma_z^2}\right) \tag{14}$$

The values of ε_y and ε_z are determined from the mass flow deficit rate immediately behind the turbine's rotor at x_a by equating that predicted by the top-hat model 7 and to the expression from the Gaussian model 14, providing the following relation:

$$\frac{D_a H_a}{2} \left(1 - \sqrt{1 - \frac{2C_T}{\beta}}\right) = 2\pi D_0 \varepsilon_y H_0 \varepsilon_z \left(1 - \sqrt{1 - \frac{C_T}{2\pi \varepsilon_y \varepsilon_z}}\right) \tag{15}$$

Hence, ε_y and ε_z expressions for VAT wakes are determined as

$$\varepsilon_y \varepsilon_z = \frac{\beta}{4\pi} \tag{16}$$

Note that the initial wake expansion rates are just a function of β , i.e. only depends on the thrust coefficient C_T . The lack of an extensive experimental

campaign focused on VAT far-wakes prevents from individually accounting for each of these wake expansion rates. Hence, for simplicity, we assume the normalised wake onset width is identical in the horizontal and vertical directions, i.e. $\varepsilon_y = \varepsilon_z$, with their value becoming

$$\varepsilon_y = \varepsilon_z = \frac{1}{\sqrt{4\pi}} \sqrt{\beta} \quad (17)$$

It is noteworthy that our formulation of the wake onset width (17) differs from the definition $\varepsilon = 0.25\sqrt{\beta}$ proposed by Abkar and Dabiri [19] and Abkar [28], which corresponds to the value for HATs. Our formulation overcomes limitations from these models in relation to non-physical estimations of ΔU at short distances behind the turbines, which resulted from an incorrect definition of ε in 14. Comparing $\varepsilon \approx 0.282\sqrt{\beta}$ (17) and $0.25\sqrt{\beta}$, the latter is approx. 12% smaller, thus leading to an underestimation of the wake onset width at $x = x_a$.

4. Prediction of the wake models

We present the validation of the wake models in four cases with comparisons to laboratory experiments, field data, and large-eddy simulations. Results from the Gaussian wake model by Abkar [28], whose underlying physics were partially based on HATs, are also included to compare the accuracy and reliability of both model predictions. From hereafter, the origin of coordinates are at the turbine centre of rotation and mid-height and for simplicity the turbine diameter and height are represented by D and H instead of D_0 and H_0 .

4.1. Single VAWT operating in a turbulent boundary layer flow

Cases 1a to 1c correspond to a single VAWT operating in a turbulent boundary layer flow representing three scenarios in which the device attains different Tip-Speed Ratios (TSR), thrust coefficient (C_T), and aspect ratio [28]. In cases 1a and 1b, the turbine has a diameter $D = 26$ m with a height $H = 24$ m whilst in case 1c its height is equal to 48 m, which yields diameter-to-height aspect ratios close to unity for former cases and almost of two for case 1c. We are interested in comparing cases 1a and 1b as the VAWT operates at TSR of 3.8 and 2.5 respectively, attaining thrust coefficients of 0.65 and 0.34 that lead to different wake dynamics. In case 1c, the turbine has a C_T equal to 0.64 and operates at $\text{TSR} = 3.8$, as in case 1a, but its

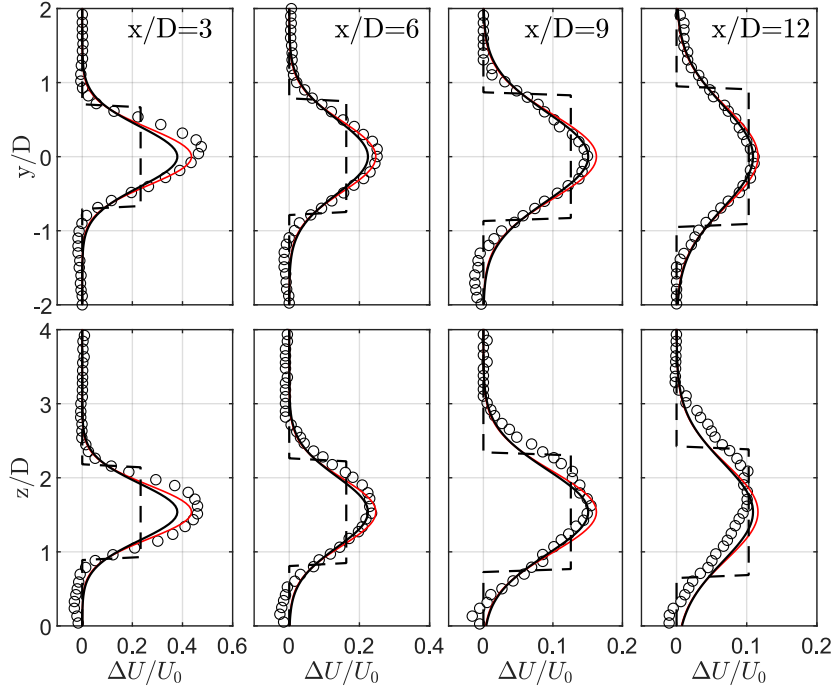


Figure 2: Normalised velocity deficit profiles for case 1a with $C_T = 0.65$, $\text{TSR} = 3.8$, $D = 26$ m and $H = 24$ m. Comparison of our proposed top-hat (dashed line) and Gaussian (solid black line) analytical wake models, with the Gaussian model proposed by Abkar [28] (solid red line) and LES-ALM results from Abkar and Dabiri [19] (circles).

aspect ratio of two promotes a larger wake asymmetry when comparing its recovery over the horizontal and vertical directions. Turbines are equipped with three NACA 0018 blades with a chord length $c = 0.75$ m, leading to a solidity value $N_b c / \pi D_0 \approx 3\%$. The free-stream velocity at hub-height (U_0) is 7.0 ms^{-1} with a turbulent intensity (I_u) of 9.1%.

Validation of normalised velocity deficit predictions obtained with the proposed analytical wake models are presented in Fig. 2 with horizontal (y) and vertical (z) profiles across the turbine wake centre at downstream distances of $x/D = 3, 6, 9$ and 12 . For completeness, we include the LES-ALM results from Abkar and Dabiri [19]. Our Gaussian model provides a similar accuracy to that of Abkar [28] at most profiles, with ours with a slight underprediction of $\Delta U/U_0$ for $x/D = 3$ observed in both vertical and horizontal profiles. Note that the model from Abkar [28] slightly overpredicts the LES-ALM velocity deficit values at the wake centre at distances of $x/D =$

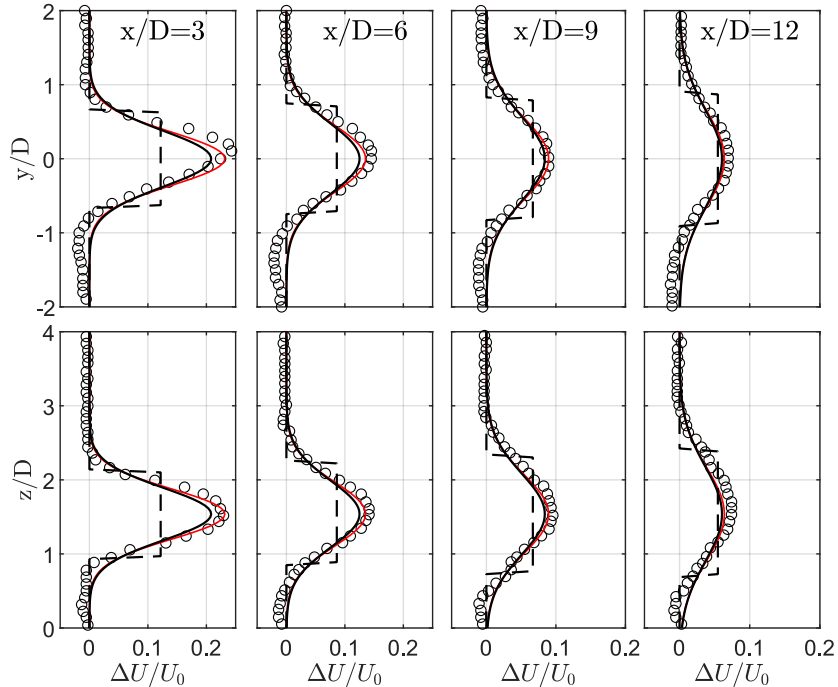


Figure 3: Normalised velocity deficit profiles for case 1b with $C_T = 0.34$, $\text{TSR} = 2.5$, $D = 26$ m and $H = 24$ m. Same legend as Fig. 2.

9 and 12, whereas ours attains a closer match to the LES data.

Figure 3 presents the results obtained for case 1b in which the VAWT operates at a lower TSR which decreases its C_T in comparison to case 1a (and case 1c). We observe our Gaussian wake model provides again a good estimate of the maximum velocity deficit at the wake centre over the vertical and horizontal directions, and the wake width is also in agreement with the LES and wake model from Abkar [28]. As VAWT wakes asymmetry depends on its aspect ratio [14], in cases 1a and 1b this is approx. unity leading the wake to feature a Gaussian distribution over the horizontal and vertical directions at $x/D \geq 3$, which supports the self-similarity assumption. Some degree of asymmetry in $\Delta U/U_0$ is appreciated at $x/D = 3$ with its maximum value over the horizontal plane being slightly larger than in the vertical one.

The turbine in case 1c has an aspect ratio close to two that promotes an uneven recovery over the vertical and horizontal directions which is well observed in Fig. 4 with the distribution of $\Delta U/U_0$ over the y -direction profiles attaining a Gaussian profile whilst, over the vertical direction, the profiles

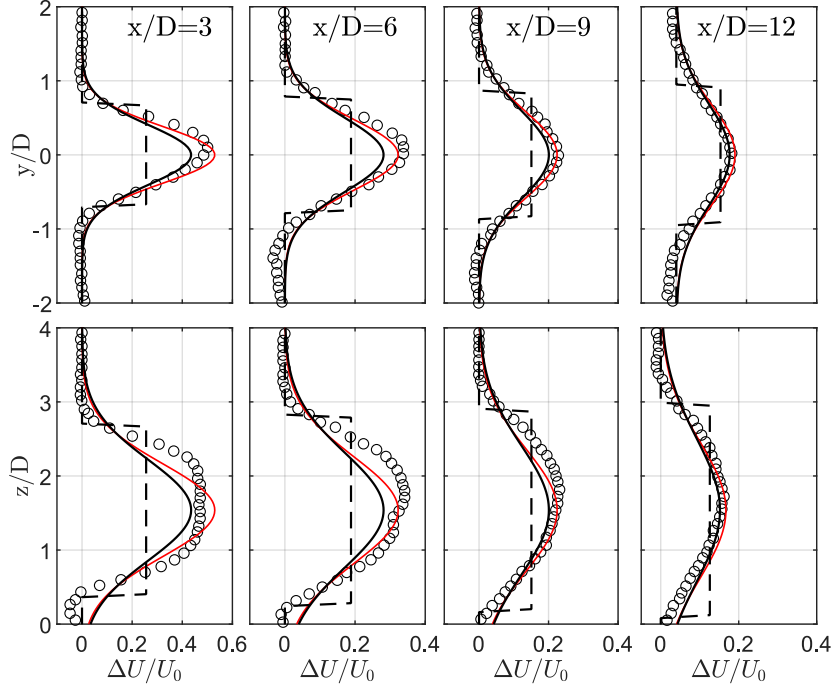


Figure 4: Normalised velocity deficit profiles for case 1c with $C_T = 0.63$, $\text{TSR} = 3.8$, $D = 26$ m and $H = 48$ m. Same legend as in Fig. 2.

nearer to the VAWT exhibit an almost top-hat distribution. After $x/D = 9$ which corresponds to $x/H = 4.5$, the LES data indicate the velocity deficit in the VAWT wake over the vertical direction recovers the Gaussian distribution. Our Gaussian wake model provides a satisfactory representation of $\Delta U/U_0$ as at $x/D = 3$ its maximum value is closer to the LES data than the one predicted by the model from Abkar [28] which overpredicts this value. Far downstream of the turbine, at $x/D = 9$ and 12, our wake model achieves a good agreement with the LES results for the maximum velocity deficit.

Further analysis of the wake predictions is presented in Fig. 5 with the evolution of maximum velocity deficit ($\Delta U_{max}/U_0$) over the streamwise direction for cases 1a to 1c, which represents the velocity scale adopted in the wake model adopted in the Gaussian and top-hat velocity distributions. In comparison to the LES results, our Gaussian model estimates a faster velocity recovery, i.e. lower maximum wake velocity deficit, than that from Abkar [28], which is a result of the considered rectangular wake onset area at x_a represented by ε_y and ε_z . For cases 1a and 1b, all analytical models

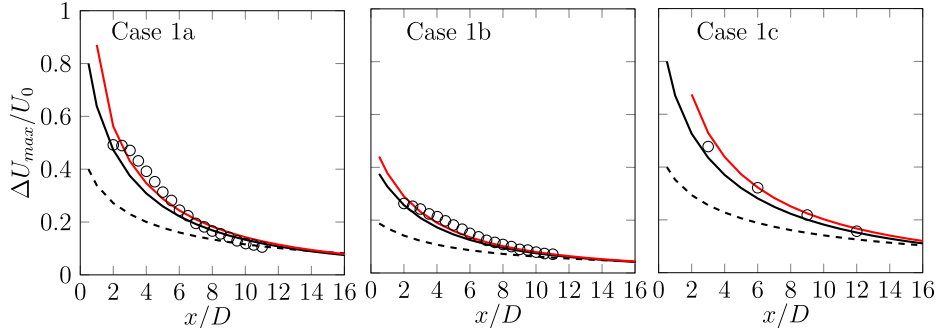


Figure 5: Normalised maximum velocity deficit for cases 1a to 1c. Same legend as in Fig. 2.

predict similar values of $\Delta U_{max}/U_0$ for distances $x/D_0 \geq 8$. Slightly larger differences are observed for case 1c in which the wake is more asymmetric, with our Gaussian analytical wake model providing a closer prediction to those from the LES. We also note that the latter is able to provide wake velocity values at any streamwise distance even immediately downstream of the VAWT, whilst Abkar [28] model fails at providing physical values for $x/D \leq 2.0$ in case 1c due to determining the value of β partly based on HAT wake characteristics.

In turbine array modelling, any analytical wake model needs to provide an accurate downstream evolution of the wake deficit so wake-to-wake interactions are reliably accounted for, which is key to estimate the performance of the individual devices as power scales according to $P \propto U_0^3$. Fig. 6 presents the streamwise evolution of the normalised total momentum deficit at the centre planes of the wake, i.e. computed over the horizontal (M_y) and vertical (M_z) directions at $z = 0$ and $y = 0$ respectively, which result from combining 3 and 4, as

$$M_i = \frac{2 \int U_w (U_0 - U_w) dx_i}{A_0 U_0^2} \quad (18)$$

An overall good agreement of the total momentum deficit is observed with the Gaussian models providing a closer match with the LES data, except for M_y in case 1a with our top-hat model attains a better match. In line with the maximum velocity deficit results, our Gaussian model predicts lower total momentum deficit which appear closer to the LES data compared to the estimates from the other theoretical models. LES results from case 1c

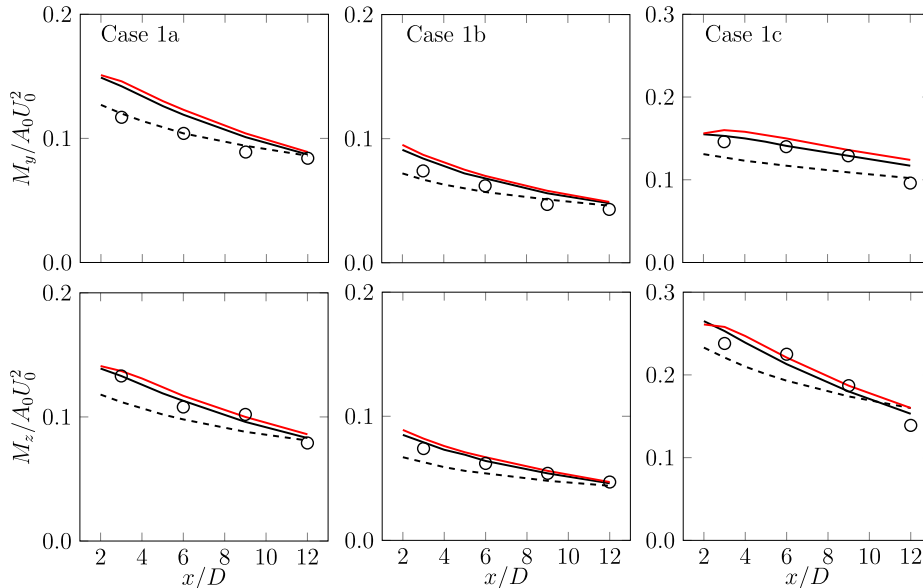


Figure 6: Predictions of momentum thickness for cases 1a, 1b and 1c. Same legend as in Fig. 2.

depict the asymmetric wake distribution with larger values for M_z than M_y , with the latter decaying at a slower rate than the vertical momentum deficit, which is well predicted by all wake models. The top-hat model appears to consistently underestimate the value of momentum deficits in most cases.

4.2. Array of four aligned VAWTs

The largest experimental facility with full-scale VAWTs, FLOWE (US), has 18 devices rated at 1.2MW and research undertaken at this site enabled the world-first quantification of a VAWT array performance and flow mechanisms driving the wake recovery [32]. To quantify the accuracy of our analytical models, we consider a configuration with four VAWTs fully aligned with the onset flow, i.e. the second to fourth turbines operate in complete waked conditions, with a separation of $11D$ between them. The turbines have a diameter and height of 1.2 m and 6.1 m respectively, with a separation of 3 m from the bottom tip to the ground level, i.e. a total height of 9.1 m, and operate at $\text{TSR} = 2.3$. The free-stream velocity is 8.45 ms^{-1} with a turbulence intensity of 11% considered for all turbines, and flow statistics in the wakes are obtained at seven equally-spaced bins that span over the

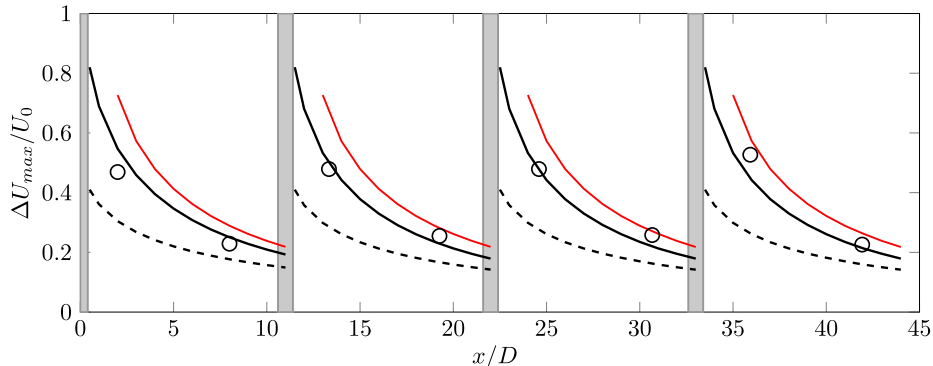


Figure 7: Normalised maximum velocity deficit profiles for the case with four full-scale VAWT. Comparison of our proposed top-hat (dashed line) and Gaussian (solid black line) analytical wake models, with the Gaussian model proposed by Abkar [28] (solid red line) and field data from Kinzel et al. [32] (circles).

whole turbine height, whose measures are then integrated into a single vertically averaged value. We estimate a thrust coefficient of 0.652 based on the field power coefficient of 0.134 calculated in Kinzel et al. [32] based on the free-stream velocity, using the induction factor of the actuator disk theory.

Comparison of the maximum velocity deficit over the centre-line of the turbines is presented in Fig. 7, including the field data which measured velocities at $2D$ and $8D$ downstream of each device, and our two proposed wake models with that from Abkar [28]. Our Gaussian wake model provides a good accuracy when compared to the field data for those points further downstream of each turbine whilst slightly over predicts the maximum velocity deficit at a distance of $2D$ downstream of the first and fourth turbine. The latter could be attributed to the wake velocity distribution not featuring full self-similarity in the wake profiles at such short distance given the aspect ratio of these VAWTs is almost of five. These results evidence the relevance of the initial wake expansion correctly accounted for in our Gaussian model compared to the one proposed in Abkar [28] which overestimates the wake velocity deficit throughout the array. Our top-hat model notably underestimates the maximum velocity deficit, in line with the results presented in §4.1, but these proved useful in the computation of the momentum thickness in the far-wake, thus somewhat valuable to predict the performance of the turbines in arrays.

A key feature of analytical wake models is that they need to provide

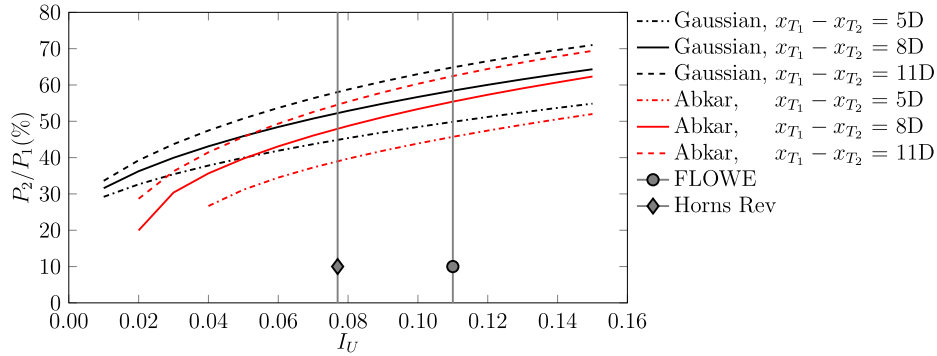


Figure 8: Evolution of the power ratio between the first two turbines at FLOWE for different levels of turbulence intensity. Comparison between our proposed Gaussian analytical wake model (black line) and that of Abkar [28] (red line).

reliable power estimates of turbines in arrays, being this dependent on the velocity field such as $P \propto U^3$. In Fig. 8 we provide a quantitative comparison of the ratio of power generated by the first turbine T_1 , assuming $U_{T_1} = U_0$, and the turbine T_2 immediately behind, with $U_{T_2} = U_w(x)$. The power ratio P_1/P_2 is estimated for various distances between these turbines, $x_{T_1} - x_{T_2}$, considering $11D$ as in FLOWE, $8D$ and $5D$, and over a range of turbulence intensities $0.01 < I_u < 0.15$ to consider scenarios representative of offshore ($I_u = 6\text{--}8\%$) or onshore ($I_u = 10\text{--}12\%$) locations [33]. Results show power production from the downstream turbine obtained with our Gaussian model is consistently larger than with Abkar’s model, in line with the evolution of velocity deficit seen in Fig. 7. Considering the well-known HAWT array of Horns Rev which can feature turbulence intensities of approx. $7\text{--}8\%$, with turbine spacing of $11D$, $8D$ and $5D$ the differences in predictions of P_1/P_2 are 6% , 9% and 14% respectively, with Abkar’s model underestimating the values as it accounts for larger velocity deficit as shown in Fig. 7. At high turbulence intensity values, variation in power estimates between models narrows down as the wake expansion increases with I_u leading to faster momentum recovery, in turn diminishing the relevance of the onset wake width prediction (Eq. 17). Overall, this power-prediction sensitivity shows that the presented improvements in our Gaussian model can avoid an underestimation of the array efficiency, especially for environments with low turbulence levels.

5. Conclusions

This paper presents a new set of top-hat and Gaussian wake models for Vertical Axis Turbines (VATs) built upon considering a rectangular wake cross-section that evolves according to two length-scales and including an asymmetric expansion over the horizontal and vertical planes. In comparison to previous wake models, we included three main features: the location at which the wake pressure is balanced is attained at $x_a = D/2$, with D being the turbine diameter; the wake at this location has a rectangular cross-section as the VAT rotor projected area that scales with a factor $\varepsilon = (\beta/4\pi)^{1/2}$; and, the asymmetric wake recovery dynamics is represented by uneven wake expansion rates.

We validated the accuracy of our proposed models in comparison to large-eddy simulation results and field data in four cases involving a standalone and an array of vertical axis wind turbines. We proved the suitability of our models to estimate the wake velocities for all cases at any downstream location, providing improvements compared to other existing VAT wake models. Our analytical models provide a good estimation of the maximum velocity deficit and momentum thickness for the three cases with a single turbine that operated at two tip-speed ratios and had two diameter-to-height aspect ratios. In application to an array of four full-scale turbines, the models compared well with field data with results showing that our Gaussian wake model attains a good estimation of the maximum velocity deficit, which verifies its reliability to predict the interaction between turbines in arrays. In relation to power generation, we performed a sensitivity analysis over a range of turbulence intensity values and turbine spacing showing there is a larger deviation between models for low turbulence values, with our Gaussian model providing larger power generation values due to its better prediction of the velocity deficit field.

Overall, the results confirmed an enhanced accuracy of our wake models compared to other previously proposed models, which will lead to improved designs of VAT arrays increasing the development pace of this promising technology.

Acknowledgements

This research was partially supported by the UK's Engineering and Physical Sciences Research Council (EPSRC) through the project EP/R51150X/1.

References

- [1] P. Veers, K. Dykes, E. Lantz, S. Barth, C. L. Bottasso, O. Carlson, A. Clifton, J. Green, P. Green, H. Holttinen, D. Laird, V. Lehtomki, J. K. Lundquist, J. Manwell, M. Marquis, C. Meneveau, P. Moriarty, X. Munduate, M. Muskulus, J. Naughton, L. Pao, J. Paquette, J. Peinke, A. Robertson, J. S. Rodrigo, A. M. Sempreviva, J. C. Smith, A. Tuohy, R. Wisser, Grand challenges in the science of wind energy, *Science* 366 (2019) 4443.
- [2] J. Liu, H. Lin, J. Zhang, Review on the technical perspectives and commercial viability of vertical axis wind turbines, *Ocean Engineering* 182 (2019) 608–626.
- [3] V. Rolin, F. Porté-Agel, Experimental investigation of vertical-axis wind-turbine wakes in boundary layer flow, *Renewable Energy* 118 (2018) 1–13.
- [4] D. Araya, T. Colonius, J. O. Dabiri, Transition to bluff-body dynamics in the wake of vertical-axis wind turbines, *Journal of Fluid Mechanics* 813 (2017) 346–381.
- [5] P. Ouro, S. Runge, Q. Luo, T. Stoesser, Three-dimensionality of the wake recovery behind a vertical axis turbine, *Renewable Energy* 133 (2019) 1066–1077.
- [6] C. M. Parker, M. C. Leftwich, The effect of tip speed ratio on a vertical axis wind turbine at high Reynolds numbers, *Experiments in Fluids* 57 (2016) 74.
- [7] A. Posa, Influence of Tip Speed Ratio on wake features of a Vertical Axis Wind Turbine, *Journal of Wind Engineering and Industrial Aerodynamics* 197 (2020) 104076.
- [8] P. Ouro, T. Stoesser, An immersed boundary-based large-eddy simulation approach to predict the performance of vertical axis tidal turbines, *Computers & Fluids* 152 (2017) 74–87.
- [9] G. Tescione, D. Ragni, C. He, C. J. Simão Ferreira, G. van Bussel, Near wake flow analysis of a vertical axis wind turbine by stereoscopic particle image velocimetry, *Renewable Energy* 70 (2014) 47–61.

- [10] G. Brochier, P. Fraunie, C. Beguier, I. Paraschivoiu, Water channel experiments of dynamic stall on Darrieus wind turbine blades, *Journal of Propulsion* 2 (1986) 445–449.
- [11] P. Bachant, M. Wosnik, Effects of Reynolds Number on the Energy Conversion and Near-Wake Dynamics of a High Solidity Vertical-Axis Cross-Flow Turbine, *Energies* 9 (2016) 73.
- [12] M. Bastankhah, F. Porté-Agel, A new analytical model for wind-turbine wakes, *Renewable Energy* 70 (2014) 116–123.
- [13] H. Kadum, R. Bayoán Cal, M. Quigley, G. Cortina, M. Calaf, Compounded energy gains in collocated wind plants: Energy balance quantification and wake morphology description, *Renewable Energy* 150 (2020) 868–877.
- [14] S. Shamsoddin, F. Porté-Agel, Effect of aspect ratio on vertical-axis wind turbine wakes, *Journal of Fluid Mechanics* 889 (2020) R1.
- [15] P. Ouro, T. Stoesser, L. Ramírez, Effect of Blade Cambering on Dynamic Stall in View of Designing Vertical Axis Turbines, *ASME Journal of Fluids Engineering* 140 (2018) 061104.
- [16] A. Posa, Dependence of the wake recovery downstream of a Vertical Axis Wind Turbine on its dynamic solidity, *Journal of Wind Engineering and Industrial Aerodynamics* 202 (2020) 104212.
- [17] A. Posa, E. Balaras, Large Eddy Simulation of an isolated vertical axis wind turbine, *Journal of Wind Engineering and Industrial Aerodynamics* 172 (2018) 139–151.
- [18] F. Porté-Agel, M. Bastankhah, S. Shamsoddin, Wind-Turbine and Wind-Farm Flows: A Review, *Boundary-Layer Meteorology* 174 (2020) 1–59.
- [19] M. Abkar, J. O. Dabiri, Self-similarity and flow characteristics of vertical-axis wind turbine wakes: an LES study, *Journal of Turbulence* 18 (2017) 373–389.
- [20] S. Shamsoddin, F. Porté-Agel, Large eddy simulation of vertical axis wind turbine wakes, *Energies* 7 (2014) 890–912.

- [21] S. Shamsoddin, F. Porté-Agel, A Large-Eddy Simulation Study of Vertical Axis Wind Turbine Wakes in the Atmospheric Boundary Layer, *Energies* 9 (2016) 366.
- [22] L. Massie, P. Ouro, T. Stoesser, Q. Luo, An Actuator Surface Model to Simulate Vertical Axis Turbines, *Energies* 12 (2019) 4741.
- [23] C. Meneveau, Big wind power: seven questions for turbulence research, *Journal of Turbulence* 20 (2019) 2–20.
- [24] P. K. Stansby, T. Stallard, Fast optimisation of tidal stream turbine positions for power generation in small arrays with low blockage based on superposition of self-similar far-wake velocity deficit profiles, *Renewable Energy* 92 (2016) 366–375.
- [25] R. J. Stevens, C. Meneveau, Flow Structure and Turbulence in Wind Farms, *Annual Review of Fluid Mechanics* 49 (2017) 311–339.
- [26] S. Frandsen, R. Barthelmie, S. Pryor, O. Rathmann, S. Larsen, J. Højstrup, M. Thøgersen, Analytical modelling of wind speed deficit in large offshore wind farms, *Wind Energy* 9 (2006) 39–53.
- [27] H. Tennekes, J. Lumley, *An First Course in Turbulence*, The MIT press, 1972.
- [28] M. Abkar, Theoretical modeling of vertical-axis wind turbine wakes, *Energies* 12 (2019).
- [29] T. Stallard, T. Feng, P. K. Stansby, Experimental study of the mean wake of a tidal stream rotor in a shallow turbulent flow, *Journal of Fluids and Structures* 54 (2015) 235–246.
- [30] M. Bastankhah, F. Porté-Agel, Experimental and theoretical study of wind turbine wakes in yawed conditions, *Journal of Fluid Mechanics* 806 (2016) 506–541.
- [31] C. R. Shapiro, D. F. Gayme, C. Meneveau, Modelling yawed wind turbine wakes: a lifting line approach, *Journal of Fluid Mechanics* 841 (2018) R1.
- [32] M. Kinzel, Q. Mulligan, J. O. Dabiri, Energy exchange in an array of vertical-axis wind turbines, *Journal of Turbulence* 14 (2012) N38.

- [33] R. J. Barthelmie, S. T. Frandsen, M. N. Nielsen, S. C. Pryor, P. E. Rethore, H. E. Jrgensen, Modelling and measurements of power losses and turbulence intensity in wind turbine wakes at Middelgrunden offshore wind farm, *Wind Energy* 10 (2007) 517–528.